

Experimental Study of Crushed Granular Materials by the Notion of Fractal Dimension in 2D and 3D.

Houria BOUZEBOUDJA (✉ bouzeboudjah@gmail.com)

Universite Mouloud Mammeri de Tizi Ouzou <https://orcid.org/0000-0003-2407-551X>

Bachir MELBOUCI

Universite Mouloud Mammeri de Tizi Ouzou

Aldjia BOUZEBOUDJA

Universite Mouloud Mammeri de Tizi Ouzou

Research Article

Keywords: Granular materials, Crushing, Mechanical tests, Fractal dimension, 2D and 3D

Posted Date: July 6th, 2021

DOI: <https://doi.org/10.21203/rs.3.rs-191072/v1>

License:  This work is licensed under a Creative Commons Attribution 4.0 International License.

[Read Full License](#)

Experimental Study of Crushed Granular Materials by the Notion of Fractal Dimension in 2D and 3D

Houria BOUZEBOUDJA*, Bachir MELBOUCI, Aldjia BOUZEBOUDJA

Geomaterials Laboratory, Environment and Development, Mouloud Mammeri University of Tizi-Ouzou, 15000, Algeria

***Corresponding author:**

Name: Houria BOUZEBOUDJA

Address: Geomaterials Laboratory, Environment and Development, Mouloud Mammeri University of Tizi-Ouzou, 15000, Algeria

Phone: +213 669 011 608

Email: bouzeboudjah@gmail.com

Abstract

The micro-texture of the aggregates of a pavement layer has a direct influence on their resistance. Whatever the position of these aggregates in a pavement structure, they must withstand, during construction or during life, the stresses of attrition and impact. In this study, a series of mechanical tests (Proctor, Los-Angeles and Micro-Deval) are carried out on grains of local materials (limestone and shale), the degree of crushing of the grains has been quantified using the concept of fractal dimension.

The fractal dimension was calculated for the different grains constituting the samples before and after each test, with the use of two two-dimensional 2D methods (Masses Method at the scale of a sample and the Box Counting Method at the scale of a grain) and a three-dimensional 3D method (Blanket on a grain scale) which is based on the use of the difference between erosion and dilation. We seek to determine from these methods the correlation between the two fractal dimensions, namely 2D and 3D and study the influence of different parameters on the mechanical characteristics of the materials chosen: the shape and size of the grains, the presence or absence of water, the stress intensity as well as the nature of the material.

The results obtained show that the three-dimensional method has a positive effect on the description of the 3D microstructure of the surface of the grains subjected to the various mechanical tests.

Key words: Granular materials; Crushing; Mechanical tests; Fractal dimension; 2D and 3D.

1. Introduction

The shape, size and texture of the grains have an influence on the mechanical behaviour of well-recognized granular materials. In the road sector, these characteristics affect hardness, durability, rigidity, tensile strength, shear strength, response to fatigue, etc. In fact, the more the size of the grain increases, the more the probability of presence of areas of weakness in the latter increases. Indeed, the more the grain size increases, the more the probability of the presence of areas of weakness in this grain increases. Microcracks extend when the grains are subjected to a high load, thus constituting an important cause of grain breakage. We can simulate the degradation of the grains in the case of the road domain by tests (LA, MDE, fragmentability, degradability, Proctor and shear) in the laboratory. The purpose of this work is to use the notion of the fractal dimension to evaluate the crushing rate of the grains of granular materials (shale and limestone) according to their hardness while knowing that the characteristics of road tests have an influence on the fractal dimension of the grains of the materials used.

According to B. Mandelbrot, the fractal dimension is, in a broad sense, "a non-integer real number ($0 < FD < 3$) which measures the degree of irregularity or fragmentation of a geometric structure or a very irregular, whose shape or pattern is found on all observation scales or the measurement of the roughness of a surface; number which, in the case of Euclidean geometric objects, is reduced to the traditional dimension (Secrieru 2009). In fact, the dimensions are whole in Euclidean geometry (1, 2 and 3), while they are irrational for fractal objects. So in fractal geometry, the dimension of a series of points on a line will be between 0 and 1, that of an irregular and plane curve will be between 1 and 2, and that of a surface full of convolution will be between 2 and 3. The fractal dimension will therefore make it possible to quantify and measure the shapes and geometries, thus highlighting the universality of these shapes.

The calculation of the fractal dimension is one of the main characteristics of fractal geometry, it has been used among others in the field of civil engineering where it finds several applications, formation of aggregates during hydration (Ji and al. 1997; Biggs and al. 1998), study of the artificial or

natural fragmentation of rocks and soils (Perrier and Bird 2002; Perfect 1997; Rieu and Perrier 1997; Inaoka and Ohno 2003; Turcotte 1997), soils study (Perrier and al. 1999; Xu 2003), etc. This fractal dimension is a number that can correspond to the characterization of the degree of compactness related to the arrangement of particles or grains, in the particular case of fracture surfaces, it can also correspond to a measurement of the roughness.

The complexity of this calculation is due to the fact that the grains of the soil are differentiated by their shape, size, and orientation. So the latter can be differently associated and related, their masses can form complex and irregular configurations which are in general extremely difficult to characterize them in geometrically exact terms (Hillel 1982).

New image analysis theories such as calculating the fractal dimension (Mandelbrot 1983) are used in this study. They are used to quantify and study the variation in crushing of the grains of the different samples studied by varying several parameters.

2. Calculation methods for the fractal dimension

Founder Mandelbrot has developed several fractal mathematical models for the purpose of calculating the fractal dimension. For the case of a surface, this dimension gives us an idea of the degree of its roughness.

There are several methods for calculating the fractal dimension, each method has its own theoretical bases. These diversities often lead to obtaining different dimensions by different methods for the same object. Although they are all different, the basic principles for calculating the dimension are always the same, they are summarized as follows:

- Measure the volume occupied by the object using different "measures".
- Plot the logarithm of the quantities measured as a function of the logarithm of the sizes and approximate this line by linear regression.
- Estimate the fractal dimension (FD) as being the slope of the line obtained best suited.

These various methods can be grouped into three classes according to this measurement principle: those based on counting boxes; those based on fractional Brownian motion; and those based on an area measurement.

Even today most of the fractal geometry calculations have been tested only in 2D (Arasan and al. 2011; Chouicha 2006; Xu 2003; Inaoka and Ohno 2003; Bouzeboudja and Melbouci 2016). There are still few applications regarding their use on 3D images. 2D analysis is limited because it only allows the study of a single facet in a location and from a particular angle of view of this complex 3D structure. So, considering volume only through a set of projection planes results in the loss of information.

Among the methods that have been extended in 3D, we find the algorithm of “differential counting of boxes” which belongs to the first class (counting of boxes), that of “variance” which belongs to the second class (fractional Brownian motion) and the “blanks recovery” algorithm which belongs to the third class (area measurement).

3. Use of the fractal dimension for granular materials

Knowing the volumes and surfaces of irregularly shaped grains of soil from images is a complex problem. This question has been complicated when it comes to quantification, as in the case of any measurement and in particular the calculation of fractal dimensions. Several studies have shown that these grains have a fractal appearance. Perfect and Kay (1991) conclude that fractal theory can be used to characterize the size distributions of aggregates and compare their fractal dimensions relative to different soil treatments.

Several studies have been made in this direction (study of granular materials with the fractal dimension), soils study (Perrier and al. 1999; Xu 2003), study of the artificial or natural fragmentation of rocks and soils (Perrier and Bird 2002; Perfect 1997; Rieu and Perrier 1997; Turcotte 1997), formation of aggregates during hydration (Ji and al. 1997; Biggs and al. 1998), study of cracking and breaking strength (Carpinteri and Invernizzi 2001; Lange and al. 1993) and that of porosity (Meng

1996), identification parameter of particle size distribution curves (Leconte and Thomas 1992; Ayed and al. 2003 ; Chouicha 2006) .

The shape and texture of the grains have an influence on the mechanical behaviour of well-recognized granular materials. In the road sector, these two characteristics affect hardiness, durability, rigidity, tensile strength, shear strength, response to fatigue, etc. As Euclidean geometry does not accurately describe all of these irregularities in shape and texture, it becomes essential to study these irregularities by the fractal theory. This theory uses the concept of fractal dimension (FD) as a means to describe the degree of irregularity and fragmentation of the grains by numerical values. The Box Counting method is one of the most used fractional dimensions: its popularity is largely due to its relative ease of rigorous calculation and numerical estimate. This dimension was used to assess grain degradation (Bouzeboudja and Melbouci 2016).

The fractal dimension of an aggregate can be linked to the arrangement of the particles forming it and will reflect the degree of its compactness or roughness. It can vary from 1 to 3, the value 3 corresponding to a solid structure (Tang and Raper 2002).

The fractal approach to grain fragmentation is attractive, easy to implement and can surely measure the variation in the fractal dimension of the granular structure.

This study is carried out with the aim of understanding the behaviour and the influence of certain parameters (the shape and size of the grains, the presence or absence of water, the stress intensity as well as the nature of the material) by performing mechanical tests (Proctor test, Los Angeles test and Micro-Deval test) on samples reconstituted in the laboratory by local materials (limestone and shale) ; while taking into account the phenomenon of grain crushing during these tests using the concept of fractal dimension. The fractal dimension was calculated using three methods (two in 2D and one in 3D). We seek to determine from these methods the correlation between the two fractal dimensions, namely 2D and 3D and to know if the evaluation of the fractal dimension of a grain or of a volume of grains can be obtained correctly from the analysis of a single facet of the grain

(projection) or to study the whole grain itself in 3D. In this article, we will study the link between the 3D fractal dimension of grains and the 2D fractal dimension of its projections or facets.

4. Methods used to calculate the fractal dimension of granular materials

Several methods have been developed to calculate the fractal dimension of a granular material. The most used methods for the quantification of the irregularity of the grains constituting the soil are based on two dimensional analysis techniques implemented from fractal theories. These methods are: the Masses method (Tyler and Wheatcraft 1992), Area Perimeter (Hyslip and Vallejo 1997), Line Divider (Mandelbrot 1983), Parallel Lines (Hammer 2005) and Box Counting methods (Russe and al. 1980). But the latter have shown an insufficiency in the description of the real geometric structure of the surface of the grains so that if we generate surfaces of the same shape but with increasing fractal dimensions (for example 2D and 3D) we notice an increase in the roughness of the soil. The results show that the fractal dimension in 3D is more practical for the precise description of a natural surface.

In the field of civil engineering, 3D fractal dimension studies were practically few in number until the 2000s. In recent years, this method has started to be used (Taud and Parrot 2005; Xu and Sun 2005; Legrain 2006; Yang, and Xu 2007; Arasan and al. 2010; Wang and Zhu 2016).

Analyzing the image texture of a given grain can be essential for more than one reason. We can find different regions in a grain image that are separated by their distinctive textures. To do this we use the Box Counting approach, which are used to subdivide the image into boxes of equal squares and then to calculate the fractal dimension, and the morphological approach which is extended in 3D (Blanket) and based on the use of the difference between the erosion and the expansion of each of the squares of the image after tests to calculate the fractal dimension. These two approaches have been applied in this article to quantify the irregularity and fragmentation of soil grains at the grain scale, and a third method which is the Masses method which gives us the fractal dimension using the results of the granulometric analysis of the studied sample, this dimension takes into account all the diameters of the measured sample.

❖ Masses method

The principle of the Masses method is the determination of the fractal dimension of fragmentation FD_{FR} by the relationship between the mass of the aggregate M and its size L corresponding to the radius of gyration and the maximum diameter.

$$M \propto L^{FD} \quad (1)$$

α (Alpha): means proportional to. (M proportional to L^{FD})

This method is based on the distribution of the grain sizes of the sample, after having chosen a well-defined particle size of a sample of material. Tyler and Wheatcraft developed a formula using granulometric analysis to calculate the fractal dimension of fragmentation (FD_{FR}) (Tyler and Wheatcraft 1992). This calculation method uses the mass of the screen rejection and its corresponding diameter. This equation is defined as follows:

$$\frac{M(R < r)}{M_T} = \left(\frac{r}{r_L} \right)^{3-FD_{FR}} \quad (2)$$

Where $M(R < r)$: cumulative mass of the grains; the size R is smaller than a given comparison of class r ;

M_T : total grain mass;

r : opening size of the sieves;

r_L : maximum grain size defined by the largest opening of the sieve size;

FD_{FR} : fractal dimension of fragmentation.

The fractal dimension is calculated using the following equation:

$$FD_{FR} = 3-m \quad (3)$$

With " m " is the exponent of the regression line best suited to the point cloud (Fig. 1).

Fig. 1 Determination of the DF_{FR} fractal dimension by the masses method for limestone in the soaked state before and after compaction at 75 blows

❖ Box Counting method

This method defined by Russe and al in 1980 is by far the most frequently used. The fractal dimension calculated by this method makes it possible to quantify the degree of fragmentation and therefore the variation in the dimensional distribution of the grains in the granular medium.

This method consists in dividing the image of a grain into small squares of identical dimensions (making a mesh), so the contour of the grain which passes through these boxes is counted, and we repeat the same operation but this time with boxes decreasing sizes and so on...

This method is based on the principle that the image of the grain corresponds to the number of boxes according to their sizes, this relationship is represented by the following formula:

$$N(X > x) = Kx^{-FD} \quad (4)$$

x: size of boxes;

X: linear dimension of the grains larger than the dimension *x*;

N(*X* > *x*): number of boxes;

k: proportionality constant;

FD: fractal dimension of fragmentation (Huang and Zhan 2002; Wang and al. 2006).

By plotting these values; size of the boxes as a function of the number of boxes in a logarithmic graph (Fig. 2), the fractal dimension is obtained according to the slope best suited to the regression line and can be calculated by the following equation:

$$DF = -m \quad (5)$$

m: the exponent of the line best suited to the point cloud.

Fig. 2 Application of the Box Counting method, calculation of the fractal dimension of a grain of $\Phi =$

8 mm from the limestone

The Box Counting method has the advantage of giving, at the grain scale, detailed information and more or less veritable measurements of the grain. Indeed, the fractal dimension varies not only according to the shape and the size of the grains, but also according to:

- The measurement scale (the larger the scale, the more precise the fractal dimension will be);
- The front of the grain for image taking;
- The quality of the image taken (number of pixels).

❖ The Blanket fractal dimension (3D)

The blanket fractal dimension has been historically defined by Peleg et al. (1984) in order to calculate the surface area of the grey levels and thus to estimate the fractal dimension FD of the volume. It is based on the Mandelbrot method and the work on Minkowski logic. Thus Peleg et al. (1984) considered all the points in a 3D space (the third dimension being the grey level) separated by a distance ε , and a surface covered therefore with a structuring element of thickness 2ε . The picture was like this defined by two surfaces, one called maximum and the other minimum (obtained by expansion and erosion of the image). The authors have shown the efficiency of their method of calculating the FD on small 3x3 windows, while other methods in the literature have estimated this dimension on larger windows. The advantage of considering small windows is to limit the surface used to locally represent the texture and therefore to ensure better delimitation of the contours, for example.

One of the advantages of this method is that if the image had its grey levels reversed, the estimated FD would not change. A second strong point is that the use of asymmetric structuring elements allows the identification of anisotropic structure inside the image (Chappard et al. 2001).

The principle of this method is as follows:

Let $g(x, y, z)$ be a 3D signal, and u_ε and b_ε respectively the surfaces of high and low intensities:

$$u_\varepsilon(i, j, k) = \max\{u_{\varepsilon-1}(i, j, k), \max_{|(m, n, m)-(i, j, k)|} u_{\varepsilon-1}(m, n, p)\} \quad (6)$$

$$b_\varepsilon(i, j, k) = \min\{b_{\varepsilon-1}(i, j, k), \min_{|(m, n, m)-(i, j, k)|} b_{\varepsilon-1}(m, n, p)\} \quad (7)$$

Where $g(i, j, k) = u_0(i, j, k) = b_0(i, j, k)$ and ε is the number of blanks. So the total white area is calculated by:

$$A(\varepsilon) = \frac{\sum_{i, j, k} (u_\varepsilon(i, j, k) - b_\varepsilon(i, j, k))}{2\varepsilon} \quad (8)$$

An estimate of the fractal dimension is equal to [3- the slope of the linear regression of $\log(A(\varepsilon))$ as a function of $\log(\varepsilon)$]. This method depends on the choice of ε and the FD found can vary greatly from one ε to another. It will therefore be important to take this parameter into account when using it.

The MATLAB R2009b software was used to facilitate the calculation of the fractal dimension with the Box Counting method and the Blanket method.

5. Characteristics of the materials used

Tizi-Ouzou province has several deposits of materials (limestone, shale, sandstone, etc.) located on the surface and near national roads, which makes their exploitation easy and inexpensive. Their choice is justified by the very important place they occupy in the realization of several civil engineering projects such as dams, roadways, railways, etc.

The two local materials used are extracted from the province of Tizi-Ouzou, limestone at a place called "candle bridge" located 7 km east of the capital of Tizi-Ouzou and shales are extracted from the deposit located at a locality called "Sidi naamane" situated about 13 km northwest of Tizi-Ouzou town. The results of the chemical analysis to determine the different minerals of the two materials which are grouped in Tables 1 and 2.

Table 1 Mineralogical compositions of limestone and shale material

Table 2 Chemical compositions of limestone and shale material

The petrographic study was carried out in a specialized laboratory of the National Office of Geological and Mining Research known as the Center for Research and Development (CRD) SONATRACH at Boumerdes town. These are thin section studies whose aim is to identify the petrographic and mineralogical characteristics of shale and limestone and to assess their relative importance, thus allowing a better understanding of their behaviour. The different minerals obtained from the two materials are described in Table 1.

The chemical study of shale (Table 2) reveals the presence of clay, this shows that they are sedimentary and not metamorphic rocks. The sample contains 60% of stable minerals (quartz) and around 30% of unstable minerals (Al_2O_3 , Fe_2O_3 and K_2O), which makes this material more sensitive to its degradation under stresses. In the case of limestone, we are in the presence of a rather pure calcite-dominated limestone having a chemical composition of 52% CaO and 2% MgO (Table 2); whereas a pure limestone composed entirely of calcite (100% CaCO_3) would have the chemical composition of 56% CaO and 44% CO₂ (composition of calcite). According to the classification of Folk (1959) (matrix-cement-grain), we are in the presence of allochems with grain greater than 10% and whose matrix is micrite intramicrite.

The results of the main geotechnical identification characteristics are grouped in Table 3 and the results of the aggregates tests in Table 4 for the two materials limestone and shale.

Table 3 The values of the physical characteristics of limestone and shale

Table 4 Results of the aggregates tests of the two materials

Material shale is more fragmentable than limestone: the fragmentability coefficient, FR (NF P94-066), of the two materials is less than 7, so they are not very fragmentable. The degradability coefficient, DG (NF P94-067), of the two materials (limestone and shale) is less than 5, so they are not very degradable (Table 4). The Micro-Deval coefficient (MDE) (NF P18-572) of limestone is lower than that of shale. The MDE coefficient of limestone is less than 20, so the material can be used for the road bodies (however class 10/16 can only be used for the sub-grade) (Table 4). For shale, the MDE coefficient is greater than 45, so the material is not usable either for the pavement bodies or for the form layers.

The Los Angeles (LA) coefficient for shale (NF P18-573) is slightly higher than that of limestone. The coefficients LA of the two materials are between 25 and 45, therefore these materials can only be used for the form layers (Table 4). Thus, the GTR (The Road Earthworks Guide) classifies the limestone used in the subclass R21 (hard limestone) and the shale in the subclass R61 (Hard magmatic and metamorphic rocks) (NF P 11-300).

SEM images (Scanning Electron Microscope) of limestone (Fig. 3a) show a moderately rough granular surface, a dense structure and illustrate the zones of presence of calcite (CaCO_3), dolomite ($\text{CaMg}(\text{CO}_3)_2$) and traces of siderite (FeCO_3) (in light grey it is calcite, in dark grey it is dolomite and in white it is siderite).

The images (Fig. 3b) also show rough surfaces with a sheet structure arranged in parallel layers for shale and illustrate the areas of presence of a few pyrite crystals, quartz, iron and clay with traces of apatite and titanium dioxide in the quartz (Bar: barite, Qtz: quartz, Pyr: pyrite, Fe : iron)

Fig. 3 SEM images of the materials studied, (a) limestone and shale (b)

These two materials (limestone and shale) were extracted in the form of large blocks. The latter are crushed using a hammer for large diameters and a jaw crusher for small diameters. The grains thus obtained are of irregular shape. The samples were made in such a way that each sample consists of a single grain shape. After sieving, the selection of shapes was made visually for each diameter of the two materials according to the most dominant shape during crushing (the angular shape for limestone and the elongated shape for shale) (Fig. 4).

Fig. 4 Forms of the materials used, angular for limestone (a), and elongated for shale (b)

6. Equipment and operating mode

Whatever the position of the aggregates in a pavement structure, they must withstand, during construction or during life, the stresses by attrition and by shocks. So, good recognition of the materials used (knowing the mechanical behaviour and characteristics of these materials) is essential. In this study, a series of mechanical tests was carried out on grains of local materials (limestone and shale), namely:

- Los Angeles test allowing us to measure the impact resistance of aggregates;
- Micro Deval test allowing us to measure the resistance to wear of aggregates and also their sensitivity to water;

- Another test was carried out (Proctor test) in order to improve the shear strength of the materials and better withstand the road loads: by tightening the grains, one against the other and reducing the volume of the voids between them, by expelling air, by compaction. The reduction in void volume between the grains leads to a reduction in the subsequent inflow of water, the effects of which are harmful, as well as the causes of attrition.

7. Characteristics of the Proctor test

Water content is an important parameter in soil compaction, since it can significantly modify its behaviour (Holtz and Kovacs 1991; Soulié 2005). The optimal water content depends on the compaction energy, so it may be more economical to choose a more powerful compaction than to water the material and compact it with lighter material.

The results of the Proctor tests, carried out on the two materials used in this study, showed the following curves (Fig. 5).

Fig. 5 Proctor curves of both limestone and shale material

The Proctor curve obtained has a slightly flattened appearance for limestone, which shows that it is not very sensitive to water, since a fairly large variation in humidity has little effect on dry density. Unlike the Proctor curve of shale which is slightly sharp, which means that it is more sensitive to water.

The sharper the Proctor curve, the more it will be necessary to have a water content very close to the optimum to obtain the desired density. The flatter the curve, the easier it will be to obtain the desired density.

To better highlight the influence of the water content on the crushing of the grains, three states of water contents were studied in this work (dry sample which means a sample with its natural water content, sample at the optimum Proctor and sample which was soaked for 24 hours) and three compaction energies (25 blows, 55 blows and 75 blows).

When preparing the samples, five control grains of each diameter were colored with a color distinct from the other diameters (Fig. 6a), which are positioned in each of the layers (five layers) of the modified Proctor mold (Fig. 6b). Photos were taken before and after the tests for each control grain, with a good resolution camera, in order to study their variations in size and shape during each test, by calculating their fractal dimensions with the Box Counting method in 2D and the Blanket method in 3D, which are based on image analysis techniques.

Fig. 6 The colored grains of each diameter (a), arrangement of the colored grains in the layers of the Proctor mold (b)

Also the fractal dimension of the samples was calculated with the masses method from the particle size distribution curve. A granulometric analysis is carried out for the entire sample before and after each test, this calculation method gives us the fractal dimension of fragmentation at the sample scale.

Fines have been defined as particles having a diameter less than the smallest diameter of the initial particle size distribution curve.

8. Presentation of results

The study of the behaviour of a granular material requires the characterization of aggregates which form it, these materials are part of civil engineering structures such as: pavements, foundations, dams, etc. For economic reasons, it is necessary to use as much as possible local materials in the realization of these structures. These materials are subject to climate change and high compressive stresses. Because of these charges, these aggregates fragment, causing a change in the granulometry (size and shape) of the grains, which induces a change in their mechanical characteristics.

8.1. Particle size distribution curves

The results of the tests are presented in the form of particle size distribution curves. These show that there is a big change in the granular structure as a function of the compaction energy (25 blows, 55

blows and 75 blows), of the variation of the water content (dried up, soaked and at the optimum) and of the granular class (4 / 6.3, 6.3 / 10 and 10/16) for the Los Angeles test and Micro-Deval test.

Fig. 7 Particle size distribution curves before and after Proctor test of limestone material

Fig. 8 Particle size distribution curves before and after Proctor test of shale material.

To highlight the grain crushing phenomenon, a granulometric analysis after each test was carried out and compared to the initial Particle size distribution curves. As a result of the increase in the number of blows, the curves shifted in ascending order (Figs. 7 and 8). In fact, the higher the number of blows, the more the crushing of the grains increases, regardless of the state of the material (dried up, soaked or at the optimum) and the nature of the sample (shale or limestone).

The photos taken after the tests show that the crushing of the grains took place during the tests carried out. In fact, during these tests, there was a crushing of the grains according to one or more failure modes (chipping, abrasion and fracture) (Fig. 9) defined by Troadec and Guyon (1994) (Fig. 10). This crushing resulted in a modification of the grain size, its shape and its surface condition.

Fig. 9 Real photos which represent the different modes of grain breakage after Proctor test

Fig. 10 Different modes of grain breakdown (Troadec and Guyon 1994)

Fig. 11 Particle size distribution curves before and after Los-Angeles test test for the three grain classes used of the two materials, **(a)** limestone and **(b)** shale

Fig. 12 Particle size distribution curves before and after Micro-Deval test for the three grain classes used of the two materials, **(a)** limestone and **(b)** shale.

Figs. 11 and 12 show a very large spread of the particle size distribution curves after the Los-Angeles and Micro-Deval tests, for the three particle size classes studied (4/6.3, 6.3/10, 10/16) of the two materials, shale and limestone. This spreading is the consequence of a very considerable production of fine particles having a diameter smaller than the smallest diameter of the initial particle size distribution curve, which means a significant crushing of the grains.

8.2. Results of the fractal dimension calculation

The fractal dimension was calculated for all the samples studied before and after each test with three methods (Masses method, Box Counting method and the Blanket method) using MATLAB R2009b software, to facilitate calculations, following their principles defined above.

The results of the evolution of the fractal dimension obtained after tests are analyzed, as a function of the compaction energy, the water content, the nature of the material and also the grain size.

8.2.1. Fractal dimension calculated with the Masses method (FD_{FR})

After each test, a granulometric analysis is carried out, a curve is drawn and the fractal dimension is then calculated by the masses method.

Fig. 13 Fractal dimensions of fragmentation calculated by the Masses method before and after Proctor test for limestone

The fractal dimension of fragmentation increases with the increase in compaction energy during the Proctor test, which consequently changes the grain crushing rate. The trend lines shown in Fig. 13 show a good fit of the data and the power law with a high degree of correlation $R^2 > 0.90$, the higher the number of blows, the closer the correlation coefficient R^2 is to 1, which means a better correlation between the fractal dimension and the number of blows.

Fig. 14 Evolution of the fractal dimension of fragmentation determined with the Masses method for the different water contents of the two materials (shale and limestone)

Fig. 14 shows an increase in the fractal dimension of fragmentation (FD_{FR}) with the increase in the number of blows for the different water contents (dried up, soaked and at the optimum) of the two materials (shale and limestone). Indeed, the more the compaction energy applied increases, the more there is an increase in fragmentation, generating a production of fine particles as shown by the increase in FD_{FR} in Fig. 14.

However, we note that under a low compaction energy, the variation of the fractal dimension is small. The value of the highest fractal dimension is 2,29 for a number of 75 blows for the shale

material and 1,96 for a number of 75 blows also for the limestone material. According to Turcotte (1997), a sample has reached total crushing when the fractal dimension of fragmentation is 2,5. These FD values show that the shale and limestone grains were not completely crushed even under this high number of blows, the sample experienced a significant but not total crash.

The figures also show that shale crushes more than limestone; this is due to the mineralogical composition where the shale has more than 30% of unstable minerals and the internal structure of the two materials (limestone with more than 78% of calcite being harder than shale). Indeed, Crushing increases with the percentage of unstable minerals present in the samples. Overall, the results thus obtained are consistent with the results of the Los Angeles, Micro-Deval and Fragmentability tests (Table 4).

The results of the calculation of the fractal dimension of fragmentation with the Masses method before and after Los Angeles and Micro Deval tests are shown in Table 5.

Table 5 Fractal dimension of fragmentation calculated by the Masses method before and after the Los Angeles and Micro-Deval tests of the two materials (limestone and shale)

Table 5 clearly show a very significant increase in FD_{FR} after the Los Angeles test and that for the three granular classes (4/6.3, 6.3/10 and 10/16) of the two materials studied (limestone and shale), which means a very high production of fine particles, particularly for class 10/16. This result is explained by the fact that small grains are more resistant than large grains. In fact, the more the size increases, the more the probability of the presence of the zones of weakness (or cracking) in the grain increases. The results also show that the FD_{FR} values of shale and limestone after Los Angeles tests are approximately the same, which means that the two materials have almost the same resistance to impact fragmentation.

Table 5 also shows a significant increase in FD_{FR} after the Micro Deval test (in the presence of water) for the three granular classes (4/6.3, 6.3/10 and 10/16) of the two materials studied (limestone and shale), which means a significant production of fine particles, particularly for shale material where we observe values of $FD_{FR} > 2$, which means that the material has undergone significant crushing.

While the values of FD_{FR} are less than 2 for limestone, it can be concluded that the presence of water has a fairly significant effect on the variation of the fractal dimension of the shale and therefore on its crushing; while its effect is less on limestone.

8.2.2. Fractal dimension calculated by the Box Counting method (2D) and the Blanket method (3D)

We also study the relation existing between the two fractal dimensions (2D and 3D) of the control grains already calculated in this work. We will therefore deduce the relevance of a three-dimensional fractal analysis of the entire volume of the grains and thus for its projections on a 2D plan calculated from image analysis techniques.

Fig. 15 Variation of the fractal dimension of the different layers calculated by the Blanket method (3D) for the dry state and the soaked state of the limestone material after Proctor test, under a compaction energy of 55 blows

Fig. 16 Variation of the fractal dimension of the different layers calculated by the Box counting method (2D) for the dry state and the soaked state of the limestone material after Proctor test, under a compaction energy of 55 blows

Fig. 17 Variation of the fractal dimension of the different layers calculated by the Blanket method (3D) for the dry state and the soaked state of the shale material after Proctor test, under a compaction energy of 55 blows

Fig. 18 Variation of the fractal dimension of the different layers calculated by the Box Counting method (2D) for the dry state and the soaked state of the shale material after Proctor test, under a compaction energy of 55 blows

The deviation of the fractal dimension calculated in 2D and 3D increases with increasing compaction energy whatever the layer (1st, 2nd, 3rd, 4th or 5th layer), the water content (dried up, soaked or at the optimum) and the nature of the material (limestone or shale) (Figs. 15, 16, 17 and 18). The deviation of the highest fractal dimension is obtained for the first layer (accumulation of compaction

energies of the upper layers plus the reaction of the mold) then it decreases from one layer to another depending on the depth, which means the more we go back to the upper layers the more the deviation of the fractal dimension decreases, knowing that the 1st layer is subjected to 5 times the compaction energy, the 2nd to 4 times, the 3rd to 3 times and so on.

The figs. 15, 16, 17 and 18 also show that the variation of the fractal dimension is all the more important as the grain size increases (increase in the diameter of the grains). These results are explained by the fact that the smallest grains are more resistant than the largest. Indeed, the more the size increases, the more the probability of presence of zones of weakness (or cracking) in the grain increases, these microcracks propagate when the grains are subjected to a high load.

Fig. 19 Variation of the fractal dimension calculated in 2D and 3D of the two materials, limestone and shale, after the Los Angeles test

Fig. 19 shows an increase in the deviation of the fractal dimension calculated in 2D and 3D of the three studied granular classes of the two materials (limestone and shale) after the Los Angeles tests. The deviation of the highest fractal dimension is obtained for the class (10/16) and the smallest is obtained for the class (4/6.3) for the two types of calculated fractal dimension (FD calculated by the Box Counting method (2D) and FD calculated by the Blanket method (3D)) of the two materials studied (limestone and shale). This can be explained by the presence of angularities or cracks in the large grains which can possibly favor their crushing more than the small grains which are healthier and more resistant (Ramamurthy 1969). This crushing causes an increase in the roughness of their surface parts, therefore an increase in the fractal dimension.

Fig. 19 also shows that there is practically no continuity of the FD curves in 2D (there is a drop between classes 6.3/10 and 10/16), which shows that 2D is not as precise as 3D where there is a perfect continuity of the values of the fractal dimension of the three granular classes.

For the Micro-Deval test, the fractal dimension was calculated only with the Masses method, because after the test it was impossible to distinguish the colored control grains from the other grains to photograph them (the color of the control grains has been erased by abrasion).

8.3. Influence of the water content on the variation of fractal dimension calculated in 2D and 3D of the two materials after Proctor test

Fig. 20 Variation of the fractal dimension of the first layer calculated in 2D and 3D for the three water contents of the limestone material under a compaction energy of 55 blows

Fig. 20 shows an increase in the deviation of the fractal dimension calculated with the 2D and 3D methods (Box Counting method and the Blanket method) with the increase in the size of the limestone grains and this for all the water contents studied (dried up, optimum and soaked). It is also noted that the deviation of the highest 2D and 3D fractal dimension is obtained for the grains in the dry state, the smallest deviation is obtained for the grains in the soaked state in 3D.

In 2D the FD curve in the soaked state is almost confused with the FD curve in the optimal state. We can conclude that limestone is not sensitive to water, this is due to its low absorption (often in limestones, a high absorption indicates a poor quality of aggregates) and the absence of micas-type minerals in its chemical composition.

The difference between the 2D and 3D calculated FD values of the first layer is important, this is justified by the fact that the first layer is the most stressed during compaction. The figure also shows that the spindle is restricted in 2D.

Fig. 21 Variation of the fractal dimension of the first layer calculated in 2D and 3D for the three water contents of the shale material under a compacting energy of 55 blows

Fig. 21 shows an increase in the deviation of the fractal dimension calculated with both 2D and 3D methods (Box Counting method and Blanket method) with the increase in grain size (grain diameter) of shale and this for all the water contents studied (dried up, optimum and soaked).

The deviation of the highest fractal dimension is obtained for the grains in the soaked state, the smallest deviation is obtained for the grains in the dry state. The grains in the optimum state Proctor has an intermediate fractal dimension deviation which means that the more the water content increases the more the crushing of the grains increases. This sensitivity to water is due to the presence of

laminated minerals like micas in the chemical composition of shale. So, we can conclude that the presence of water weakens the grains and reduces the resistance to fragmentation under impact during compaction. The water surrounding the grains penetrates into the microcracks and makes the fragile areas less consistent, this induces easily degradable crusts.

Fig. 21 also shows that the difference between the values of FD calculated in 2D and in 3D is reduced in the case of shale (the spindle is more loaded).

8.4. Comparative study between the fractal dimension calculated in 2D and the fractal dimension calculated in 3D

Fig. 22 Fractal dimension calculated in 2D and 3D of limestone before and after Proctor test

Fig. 23 Fractal dimension calculated in 2D and 3D of the shale before and after Proctor test

The two figs. 22 and 23 show that the values of the fractal dimension calculated with the Blanket method (3D) are higher than the values calculated with the Counting Boxes method in 2D (the values of FD in 2D are between 1 and 2, on the other hand the values of FD in 3D are between 2 and 3), which means that the 3D method takes into account all the irregularities of the grain (the whole grain) unlike the 2D method which takes into account only the irregularities of the surface on a single plane,(the more the fractal dimension increases the more the object is irregular). It is obvious that the quantity of fine particles obtained on all facets of a grain is greater than the quantity of fines obtained on a facet, which indicates the increase in FD (3D) compared to FD (2D).

The fractal dimension obtained after the Proctor test calculated in 2D and 3D is less than that before the test for practically all the diameters of the grains of limestone material (Fig. 22). This is explained by the fact that after crushing certain grains lose part of their material (rupture of the angularities), which leads to a reduction in their sizes then a modification of the shape (less irregular shape) and grain texture (less rough surface) which induces a reduction in the fractal dimension after testing.

Fig. 23 shows an increase in the fractal dimension obtained after the test calculated with the Blanket method unlike the results calculated with the Box Counting method, which show a reduction in the fractal dimension obtained after testing, because this method does not take into account the mode of rupture of shale grains which is a break throughout a grain sheet giving us fines that are produced from small pieces of sheets which remain stuck on the grain. This breaking mode leads to a reduction in the thickness of the grain which cannot be seen with the 2D method (projection on a single plane), but with the 3D method (the entire volume of the grain) we can see all the irregularities that are produced after test (increase in irregularities means an increase in FD), this explains the increase in fractal dimension calculated with the 3D method after test.

Fig. 24 Variation of the fractal dimension calculated in 2D and 3D of the two shale and limestone materials before and after Los Angeles test

During the Los Angeles tests, the samples underwent a rupture of the asperities, then an intense fragmentation, which makes the surface of the grains of the two materials (shale and limestone) rougher and many small particles were produced. Thus, it was reasonable to have higher values of the fractal dimension after testing calculated with the two methods (2D and 3D) (Fig. 24).

The arrangement of grains in a volume is a complex 3D network of grains in contact with each other. Therefore, 2D analysis is limited because it only allows the study of a single facet (on a plane) in a particular place and under a particular angle of vision of this complex 3D structure, therefore this analysis does not take into account all the irregularities which justifies the high values of the FD in 3D compared to those in 2D.

9. Conclusion

Using fractal theory, it is possible to quantify the structures of grains of complex shape through the fractal dimension which is a parameter which indicates how an irregular structure tends to fill the space after observation at different scales. The breakage of the grains depends on many factors which affect the variation of the fractal dimension, namely: the granulometry, the size, the shape and the nature of the grains; the intensity of the energy applied; and the presence or absence of water. The FD

decreases in the case of a "splitting and / or breaking of the roughness" and it increases in the case of a "chipping" which causes the increase in grain irregularities.

The results of calculation of DF in 2D and in 3D show that the projection on a single plane or a single facet of the grain is not sufficient to characterize the volume of a grain, because it provides information on this part only and not on the entire volume of the grain. Likewise, the fractal dimension of a single facet (a single plane) is not an appropriate parameter for characterizing the volume of the grain. Under the effect of a stress, the degradation of the microstructure of the grain is not limited to a single direction.

The results also show a correlation between the values of the fractal dimension calculated with the Blanket method and the values of the fractal dimension calculated with the Box Counting method. But there is no possibility, in the general case, to find an exact link between the values of the FD in 3D of the grains and the values of FD in 2D of its projections. Moreover, even if it exists, this relationship between the fractal dimension of a volume and that of its projections changes with the direction of projection.

High values of fractal dimensions are associated with a high number of blows in the Proctor test and a high water content, these high values of this dimension indicate that the sample is fractal. The presence of minerals like micas is an element of weakness for the aggregate. When they are dominant, the resistance of the aggregates is low and the sensitivity to water is pronounced.

The fractal approach of the grains of soil is interesting, easy to implement and makes it possible to measure the complex variation of the micro-architecture of the grains. It would be interesting to extend the study to other 3D fractal and multi-fractal methods in order to better quantify the total degradation of the grain.

Declarations

Funding: There is no funding, this work is part of a research project of the University of Tizi-Ouzou.

Conflicts of interest/Competing interests: This work once published can be made available to researchers. There are no conflicts of interest.

Availability of data and material: The equipment on which we worked is equipment from the Tizi-Ouzou University laboratory.

Code availability: The software used is available at the laboratory of the University of Tizi Ouzou.

Authors' contributions: The authors welcome the submission of this work and they fully agree with the publication of this article.

References

AFNOR (1990) Aggregates. Los Angeles test. NF P18-573

AFNOR (1990) Aggregates. Micro-Deval attrition test. NF P18-572

AFNOR (1992) Earthworks. Classification of materials for use in the construction of embankments and capping layers of road infrastructures. NF P 11-300

AFNOR (1992) Soils: investigation and tests. Degradability coefficient of rocky material. NF P94-067

AFNOR (1992) Soils: investigation and tests. Fragmentability coefficient of rocky material. NF P94-066

Arasan S, Akbulut S, Hasiloglu AS (2011) The Relationship between the Fractal Dimension and Shape Properties of Particles. KSCE Journal of Civil Engineering 15(7):1219-1225

Arasan S, Yener E, Hattatoglu F, Akbulut S, Hinislioglu S (2010) The relationship between the fractal dimension and mechanical properties of asphalt concrete. International Journal Of Civil And Structural Engineering 1(2):165-170

Ayed K, Chouicha K, Benaissa A, Semcha A, and Mekerta B (2003) Identification of compactness by the fractal dimension, Proceeding of the National Civil Engineering Seminar. Editions Dar El Gharb, ENSET Oran 28–29

Biggs S, Habgood M, Jameson GJ, Yan Yd (1998) The fractal analysis of aggregates formed via a bridging flocculation mechanism. Proceedings of the 26th Australian Chemical Engineering Conference, Chemeca 98, Port Douglas, Australia

Bouzeboudja A, Melbouci B (2016) Study of the evolution of the fractal dimension of a granular material's grains during mechanical tests. Bulletin of Engineering Geology and the environment 75(2):821-839

Carpinteri A, Invernizzi S (2001) Influence of damage on the fractal properties of concrete subjected to pure tension. Materials and structures 34: 605-611

Chappard D, Chennebault A, Moreau M, Legrand E, Audran M , Basle MF (2001) Texture analysis of X-ray radiographs is a more reliable descriptor of bone loss than mineral content in a rat model of localized disuse induced by the clostridium botulinum toxin. Bone 28:72-79

Chouicha K (2006) Fractal dimension and granular range as parameters for identifying granular mixes. Materials and Structures 39:665–681

Folk RL (1959) Practical petrographic classification of limestones. American Association of Petroleum Geologists Bulletin 43:1-38

Hammer KP (2005) Analysis of granular materials in Pennsylvania highways. Master of Science Thesis, University of Pittsburgh

Holtz RD, Kovacs WD (1991) Introduction à la géotechnique. Editions de l'Ecole Polytechnique de Montreal, Montreal

Huang GH, Zhan WH (2002) Fractal property of soilparticle size distribution and its application. ActePedol Sin 39:490–497

Hyslip J, Vallejo L (1997) Fractal analysis of the roughness and size distribution of granular material. Eng Geol 48(3–4):231–244

Inaoka H, Ohno M (2003) New universality class of impact fragmentation, Fractals 11(4):369–376

Ji X, Chan SYN, Feng N (1997) Fractal model for simulating the space-filling process of cement hydrates and fractal dimensions of pore structure of cement-based materials. *Cement and Concrete Research* 27 (11):1691-1699

Lange DA, Jennings HM, Shah SP (1993) Relationship between fracture surface roughness and fracture behaviour of cement paste and mortar. *J. Am. Ceram Society* 76 (3):589-597

Leconte A and Thomas A (1992) Fractal character of granular mixes for highly compact concrete. *Materials and Structures* 25:255–264

Legrain H (2006) Study of the influence of roughness on fluid flow in rock cracks. Thesis, Polytechnic Faculty of Mons

Mandelbrot B (1975) Les objets fractals, forme, hasard et dimension. Flammarion editions, Paris, p190

Mandelbrot B (1983) The fractal geometry of nature. Edition W.II. Freeman, San Francisco, p 461

MATLAB R2009b

Meng B (May 1996) Determination and interpretation of fractal properties of the sandstone pore system. *Materials and Structures* 29: 195-205.

Peleg S, Naor J, Hartley R, Avnir D (1984) Multiple resolution texture analysis and classification. *IEEE Trans, Pattern Anal, Mach. Intell, PAMI* 6:518–523

Perfect E, Kay BD (1991) Fractal theory applied to soil aggregation. *Soil science society of America journal* 55(6):1552-1558

Perfect E (1997) Fractal models for the fragmentation of rocks and soils: a review. *Engineering Geology* 48:185- 198

Perrier E, Bird N, Rieu M (1999) Generalizing the fractal model of soil structure: the pore –solid fractal approach. *Geoderma* 88:137-164

Perrier E, Bird N (2002) Modelling soil fragmentation: the pore solid fractal approach. *Soil & Tillage Research* 64:91-99

Ramamurthy T (1969) Crushing Phenomena in Granular Soils. *Journal of the Indian National Society of Soil Mechanics and Foundation Eng.* Vol.8

Rieu M, Perrier E (1997) Fractal models of fragmented and aggregated soils, in *Fractal in Soil Sciences*. Edited by Baveye, P., Parlange, J.Y. and A. Stewart, B.A., CRC Press LLC 169-202.

Secrieru C, (2009) Applications de l'analyse fractale dans le cas de ruptures dynamiques. Doctoral Thesis Mechanics and Materials, Polytechnic University of Timisoara, Romania

Russe D, Hanson J, Ott E (1980) Dimension of strange attractors. *Phys Rev Lett* 45:1175–1178

Soulié F (2005) Cohésion par capillarité et comportement mécanique de milieux granulaires. Doctoral thesis, University of Montpellier II

Tang P, Raper JA (2002) Modelling the settling behaviour of fractal aggregates, a review. *Powder Technology* 123(2-3):114-125

Taud H and Parrot J-F (2005) Measurement of DEM roughness using the local fractal dimension. *Géomorphologie: relief, processus, environnement* 4:327-338

Troadec JP, Guyon E (1994) Du Sac de Billes au tas de Sables. Editions Odile JACOB, Paris

Turcotte DL (1997) *Fractals and Chaos in Geology and Geophysics*. Second Edition, Cambridge University Press

Tyler SW, Wheatcraft SW (1992) Fractal scaling of soil particle-size distributions: analysis and limitations. *Soil Sci Soc Am J* 56:362–369

Wang C, Zhu H (2016) Combination of Kriging methods and multi-fractal analysis for estimating spatial distribution of geotechnical parameters. *Bull Eng Geol Environ* 75:413–423

Wang X, Li M-H, Lui S, Lui G (2006) Fractal characteristics of soils under different land-use patterns in the arid and semiarid regions of the Tibetan plateau China. *Geoderma* 134(1–2):56–61

Xu YF (2003) Surface fractal dimension of swelling clay minerals. *Fractals* 11(4):353-362

Xu Y F, Sun DA (2005) Correlation of surface fractal dimension with frictional angle at critical state of sands. *Geotechnique* 55(9):691-695

Yang R, Xu Z, (2007). Relationship between fractal dimension and road performance of dense-gradation asphalt mixture. *Tumu Gongcheng Xuebao/China Civil Engineering Journal* 40(3):98-103

Figures

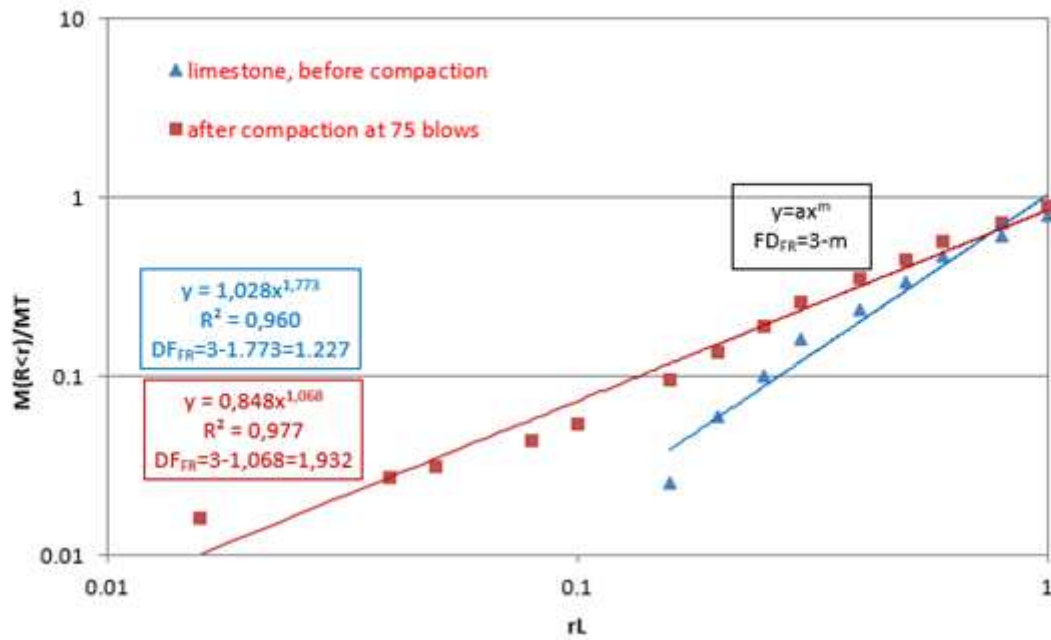


Figure 1

Determination of the DFFR fractal dimension by the masses method for limestone in the soaked state before and after compaction at 75 blows.

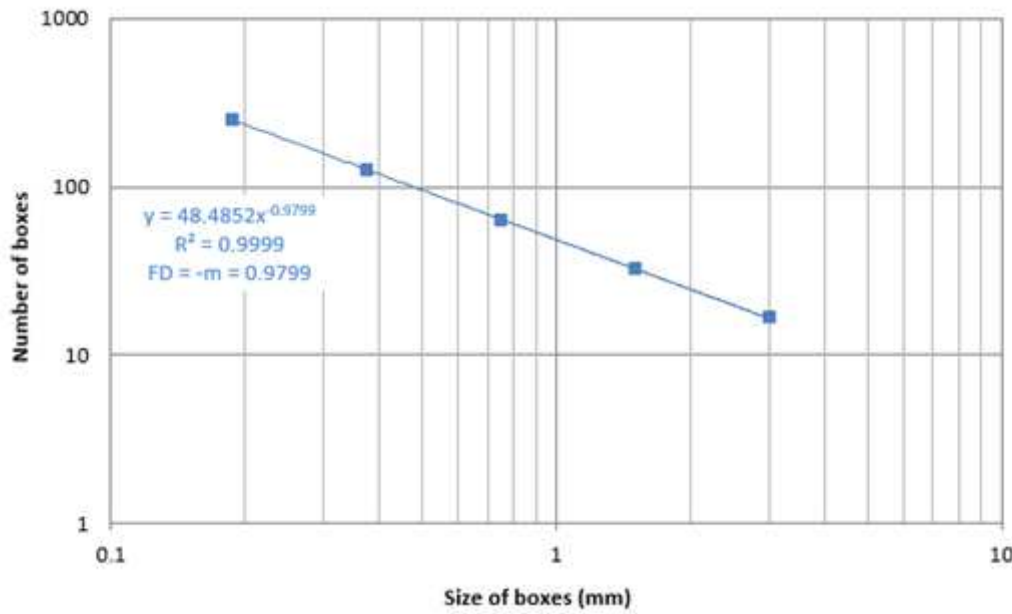
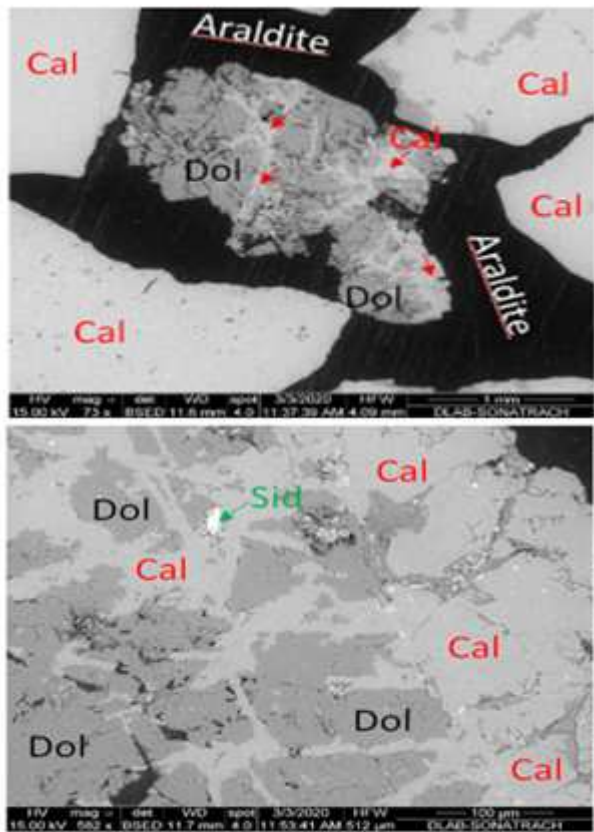
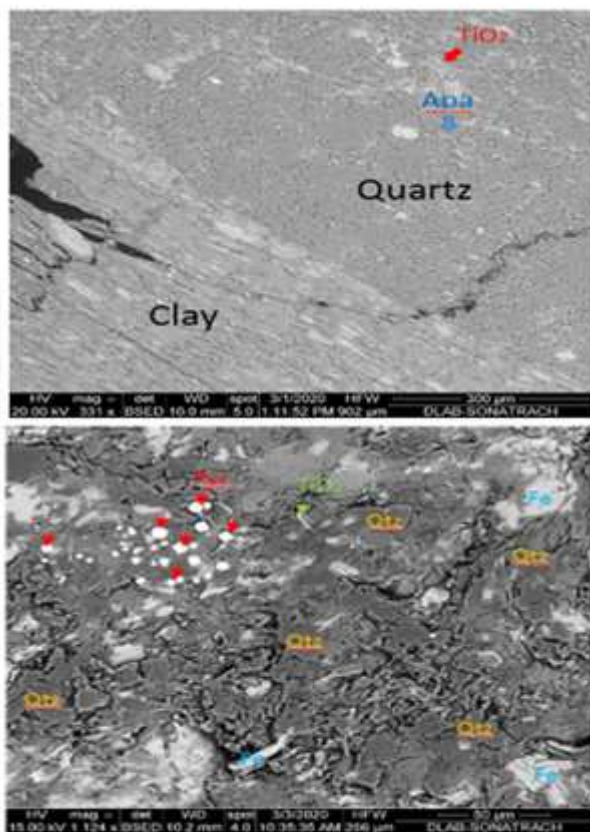


Figure 2

Application of the Box Counting method, calculation of the fractal dimension of a grain of $\Phi = 8$ mm from the limestone



(a) Limestone



(b) Shale

Figure 3

SEM images of the materials studied (limestone and shale)



Figure 4

Forms of the materials used, respectively angular for limestone and elongated for shale

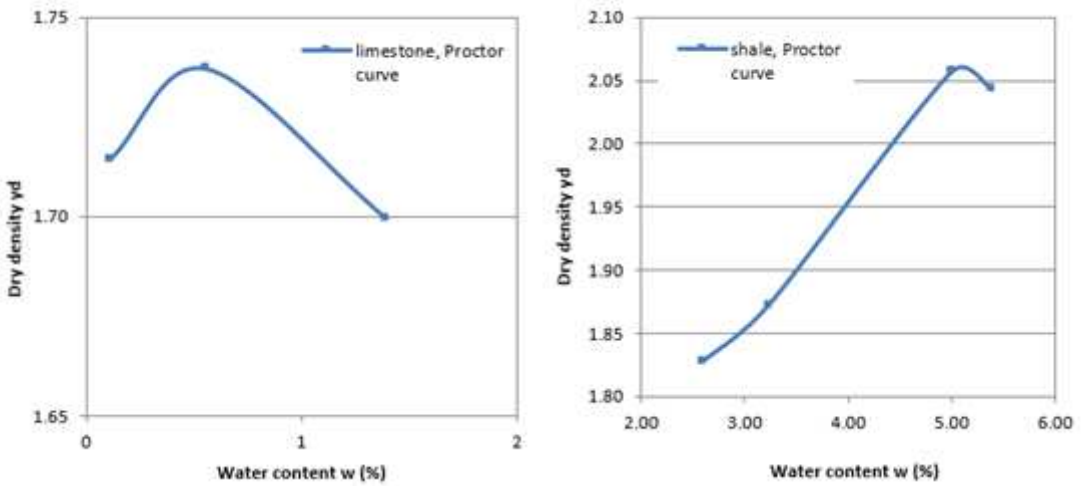


Figure 5

Proctor curves of both limestone and shale material



Figure 6

(a) The colored grains of each diameter, (b) arrangement of the colored grains in the layers of the Proctor mold

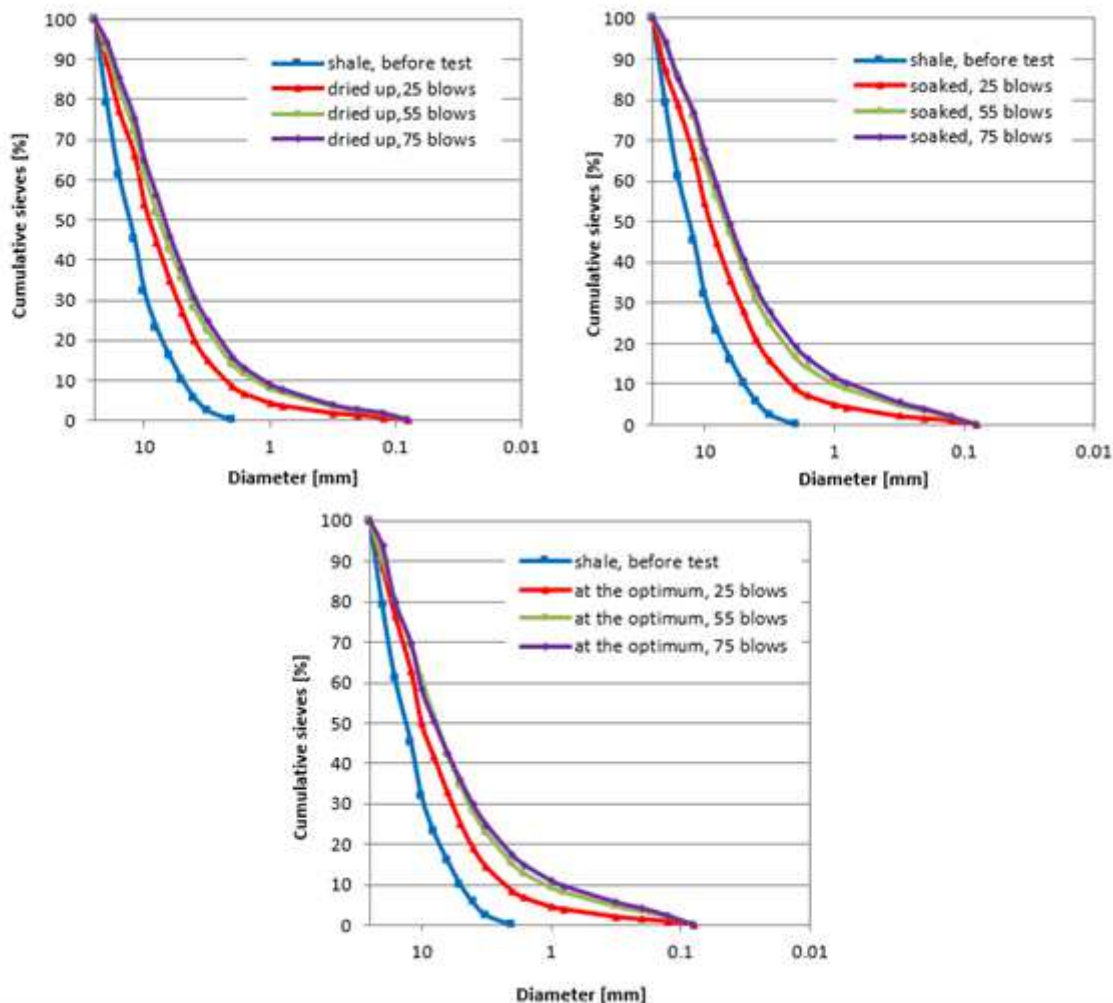


Figure 8

Particle size distribution curves before and after Proctor test of shale material.



Figure 10

Different modes of grain breakdown (Troadec and Guyon 1994)

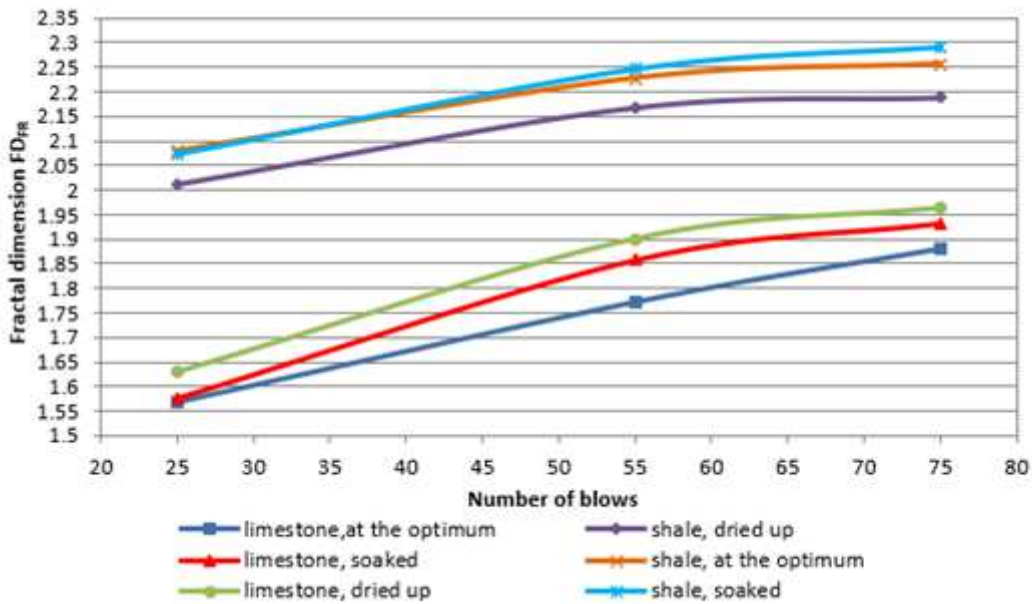


Figure 14

Evolution of the fractal dimension of fragmentation determined with the Masses method for the different water contents of the two materials (shale and limestone)

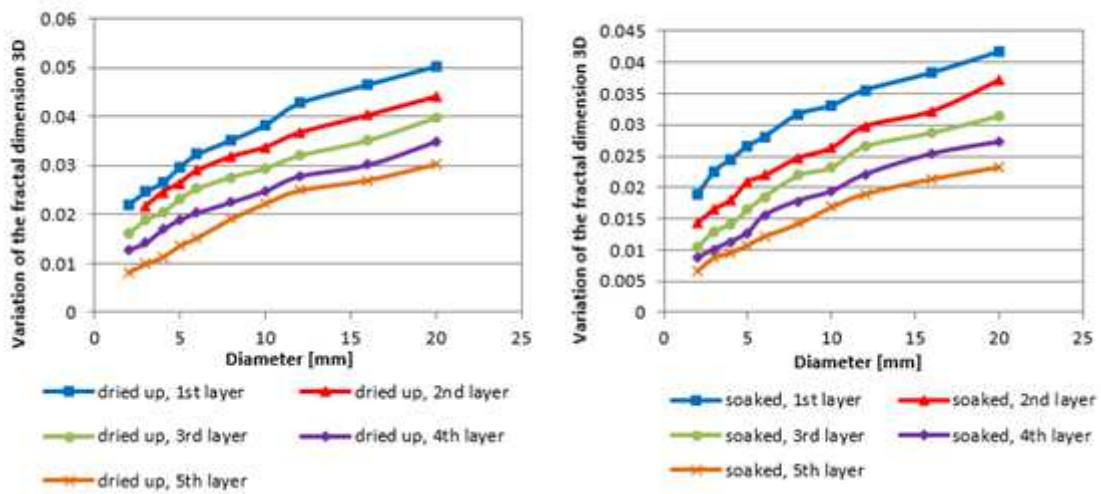


Figure 15

Variation of the fractal dimension of the different layers calculated by the Blanket method (3D) for the dry state and the soaked state of the limestone material after Proctor test, under a compaction energy of 55 blows

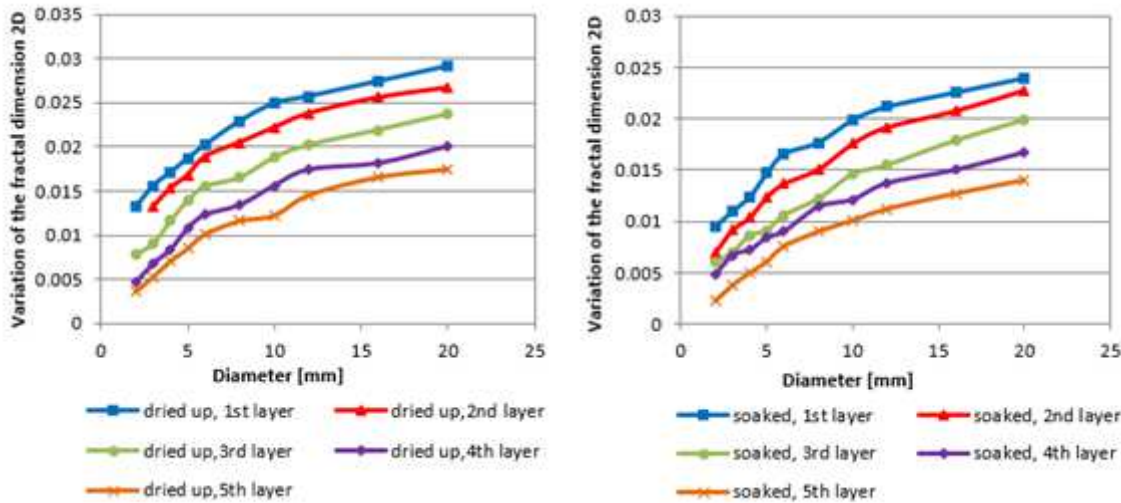


Figure 16

Variation of the fractal dimension of the different layers calculated by the Box counting method (2D) for the dry state and the soaked state of the limestone material after Proctor test, under a compaction energy of 55 blows

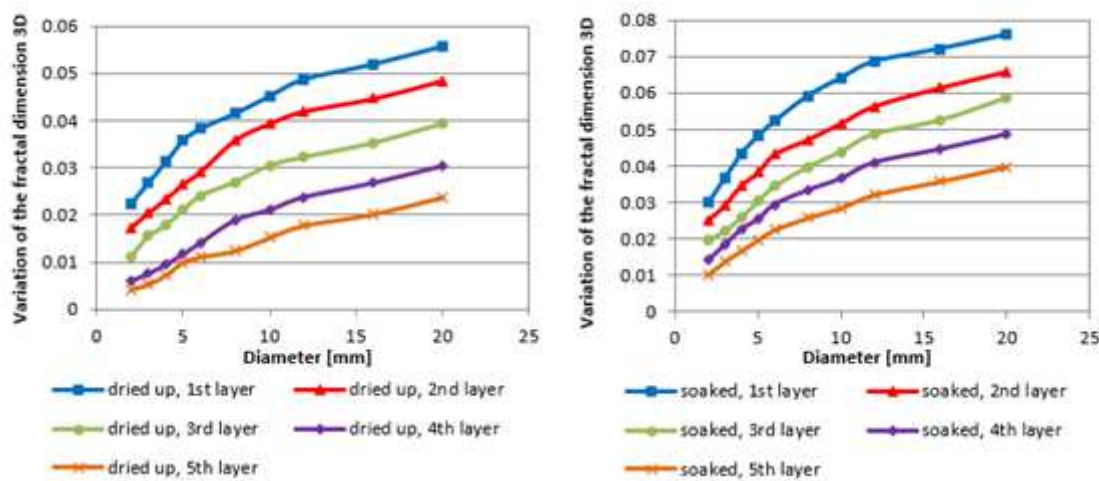


Figure 17

Variation of the fractal dimension of the different layers calculated by the Blanket method (3D) for the dry state and the soaked state of the shale material after Proctor test, under a compaction energy of 55 blows

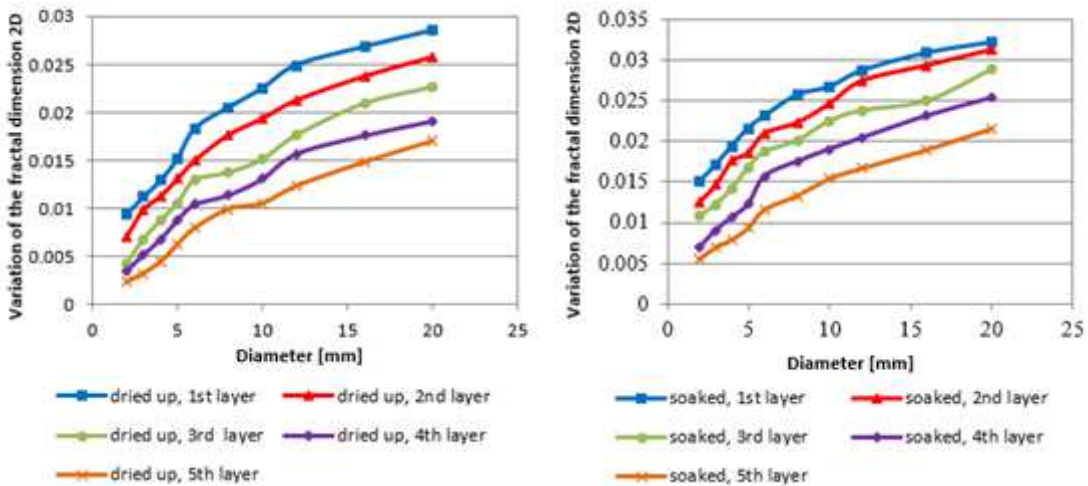


Figure 18

Variation of the fractal dimension of the different layers calculated by the Box Counting method (2D) for the dry state and the soaked state of the shale material after Proctor test, under a compaction energy of 55 blows

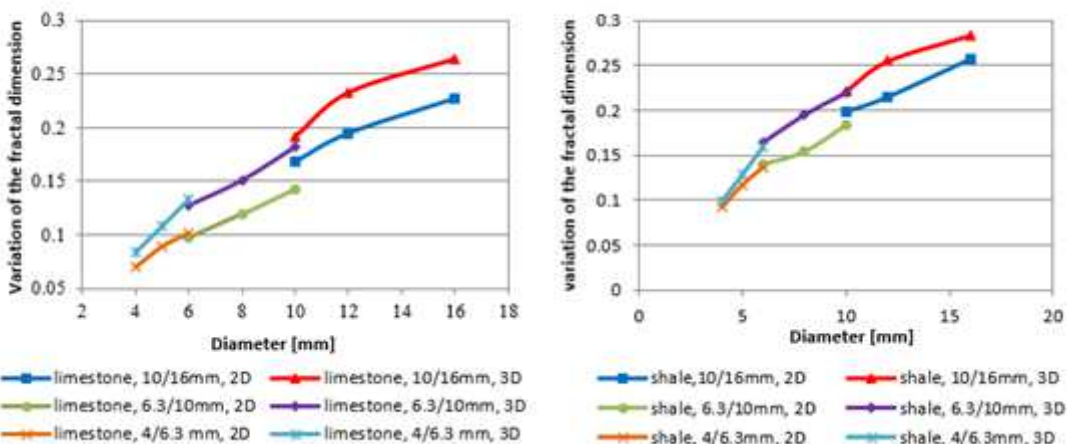


Figure 19

Variation of the fractal dimension calculated in 2D and 3D of the two materials, limestone and shale, after the Los Angeles test

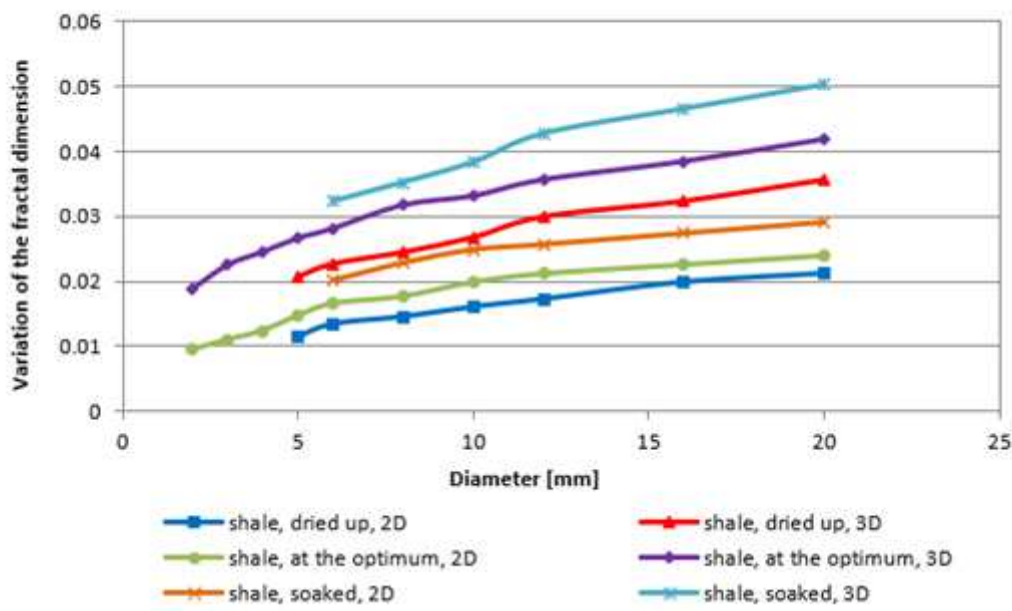


Figure 21

Variation of the fractal dimension of the first layer calculated in 2D and 3D for the three water contents of the shale material under a compacting energy of 55 blows

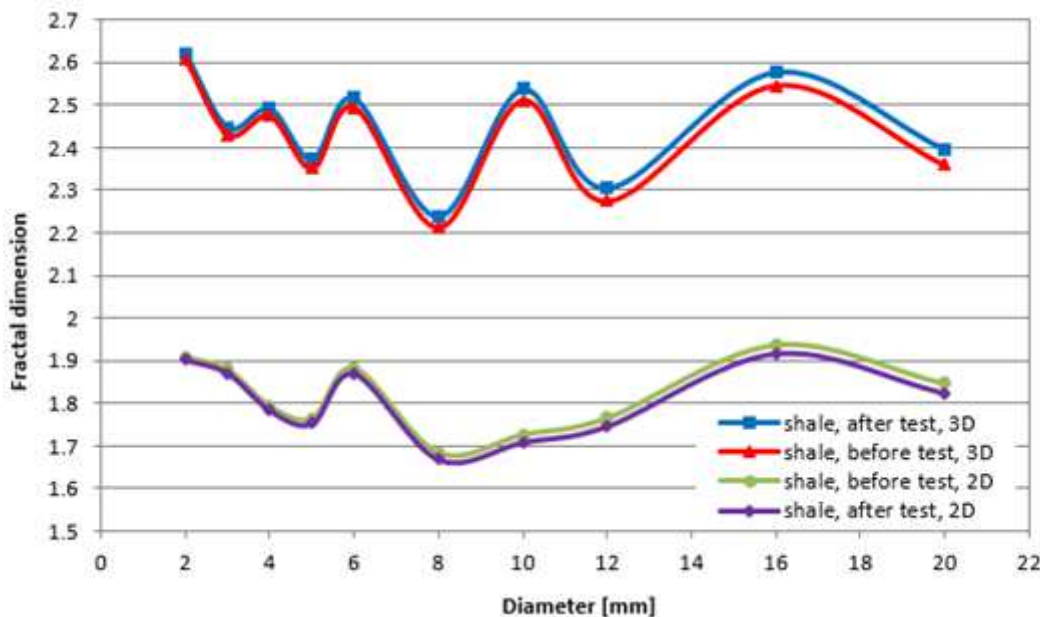


Figure 23

Fractal dimension calculated in 2D and 3D of the shale before and after Proctor test

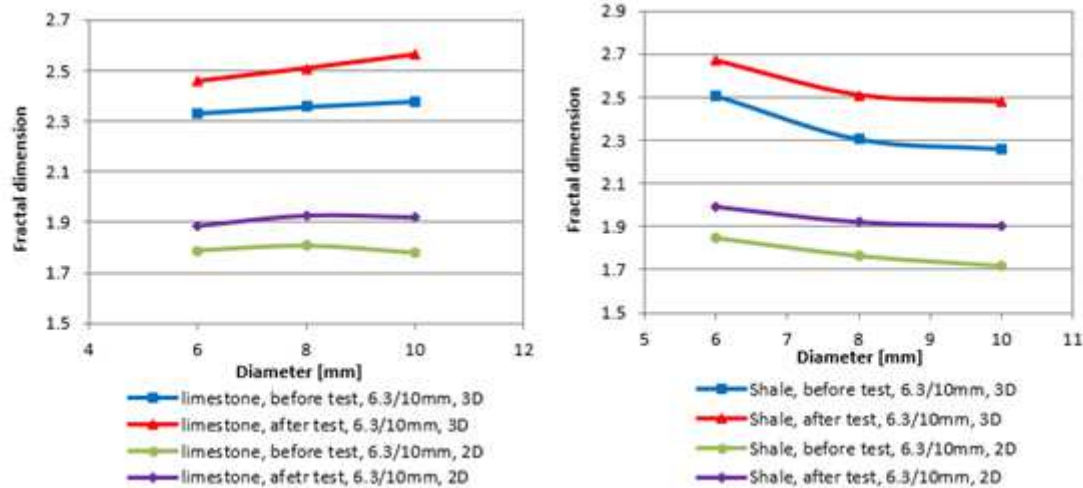


Figure 24

Variation of the fractal dimension calculated in 2D and 3D of the two shale and limestone materials before and after Los Angeles test